

The environmental properties of galaxies from the GOODS-SOUTH survey up to $z \sim$ 2.5

L. Pentericci, M. Castellano, A. Fontana, A. Grazian, S. Salimbeni,
D. Trevese and others



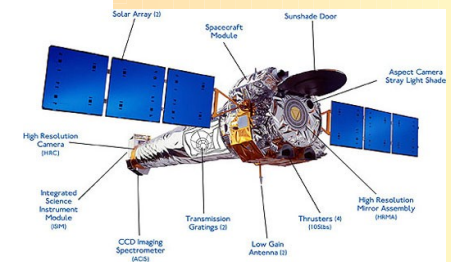
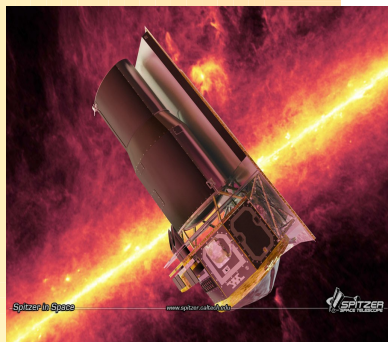
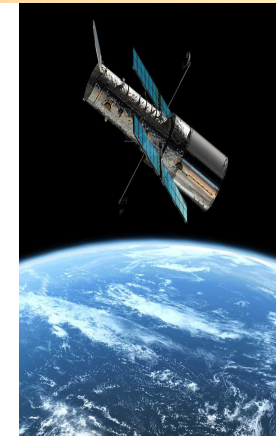
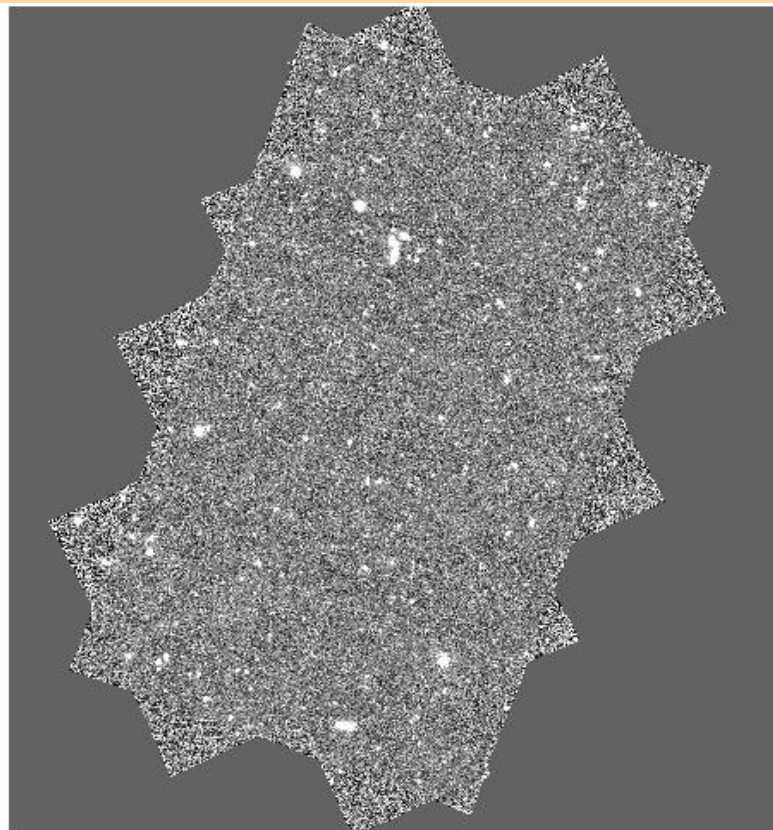
INAF - Oss. Astronomico di Roma

The GOODS Survey

The Great Observatories Origins Deep Survey covers all the Chandra Deep Field South.

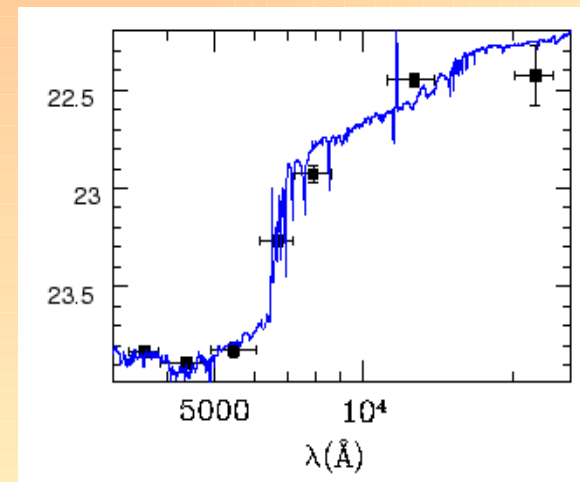
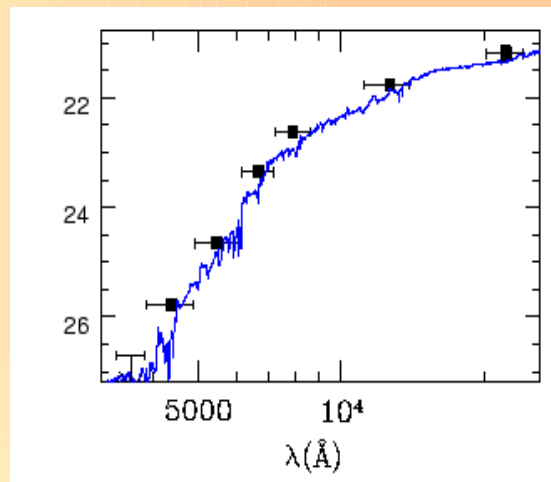
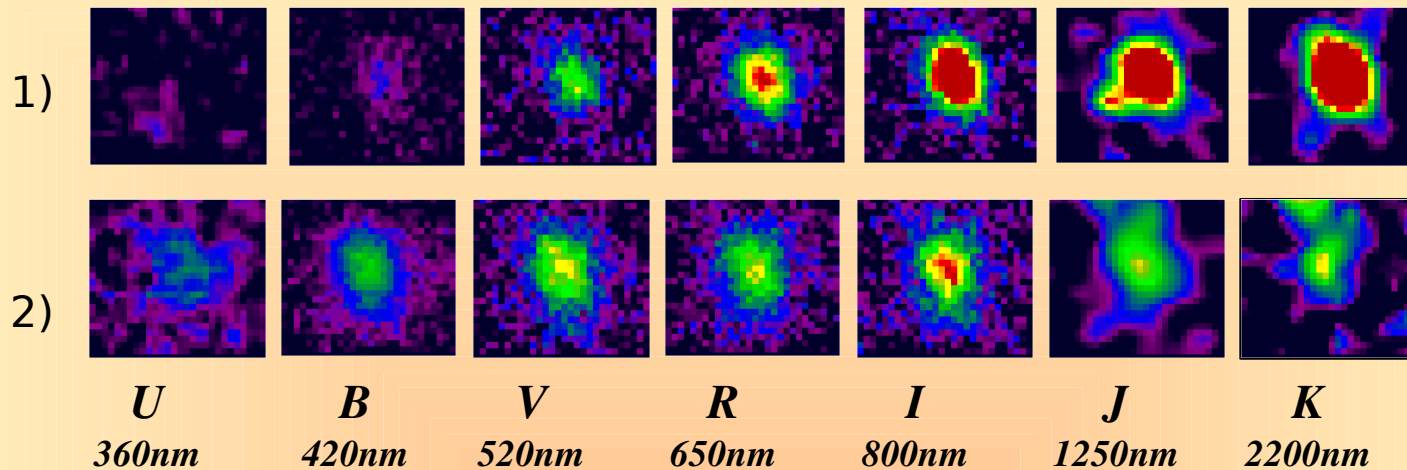
The GOODS-MUSIC catalogue (Grazian et al. 2006) uses 15 bands photometry of 14847 extragalactic objects, selected either in the z_{850} or in the K_s band to a limiting magnitude $z_{850} \sim 26$ (AB). Recently MIPS- 24 μm data have been also included (Santini et al. 09)

The field has been extensively covered by spectroscopic observations and there are more than 2000 redshift available (Vanzella et al. 2009, Popesso et al. 2009 and others)



z-band ACS image

A photometric estimate of the redshift of a galaxy can be obtained from multiwavelength data through a reconstruction of the galaxy SED (e.g. χ^2 fitting in redshift-colour space using libraries of synthetic templates):



The average dispersion of the photo-z is very low : $\langle |\Delta z / (1 + z)| \rangle = 0.03$ up to $z = 2$

Studying the evolution of galaxies using GOODS-MUSIC : an overview

- **The most distant LBGs** (Castellano et al. 2009 arXiv0909.285) *using ultradeep HAWKI Y-band observations of GOODS-South we have searched for candidate $z=7$ LBGs having $z-Y > 1$. Seven good candidates were found. The results provide evidence for a very fast evolution of the UV LF beyond $z=6$. Spectroscopic confirmation of the candidate is on-going with FORS2. Similar analysis of other two fields to double the statistics is being carried out.*
- **Properties of Lyman Break Galaxies and their dependence on the Ly α emission line** (e.g. Pentericci et al. 2007 Pentericci et al. 2009 Pentericci et al. sub) *various works to investigate how the physical and morphological properties of LBGs from $z=3$ to $z=6$ depend on the presence and characteristic of the emission line. Investigation of the relation between LBGs and Ly α emitters*
- **Star formation properties and mass assembly process at high z** (Fontana et al. 2009, Santini et al. 2009) *Study of the SF properties of galaxies from their mid IR emission. Evolution of the fraction of the star forming population vs quiescent and "red and dead" galaxies and comparison to semianalytical model predictions*

Studying the evolution of galaxies using GOODS-MUSIC : an overview

- Evolution of galaxy population as a function of color:

(e.g. Salimbeni et al. 2008) derivation of LF and luminosity density as a function of redshift for blue/late and red/early populations. The bimodality in the U-V color and specific star formation rate is observed up to $z=3$. The shape of the red/early LF shows an excess of faint red dwarf galaxies

A Wide and ultra Deep survey for LBG at $z=3$: the slope of the UV luminosity function. *(Boutsia et al. In preparation) Using ultra deep UGRZ images over 0.5 sqdeg of several fields including some of the Steidel fields with spectroscopy we estimate the observational uncertainties involved in the selection of candidates and in the evaluation of the UV luminosity function at the faint end.*

Studying the evolution of galaxies using GOODS-MUSIC: an overview

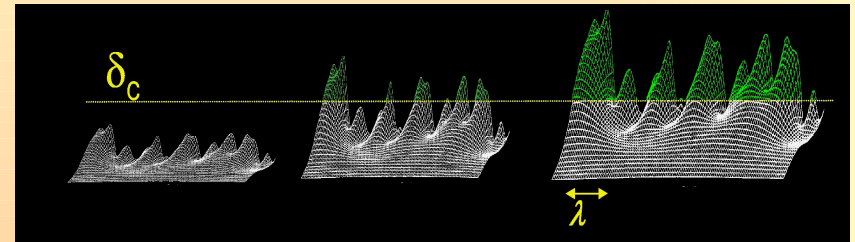
A search of clusters/large scale structures in the GOODS- South field using accurate photometric redshift

A statistical analysis of the physical and observational properties of galaxies (SFR color age mass) and their dependence on the environmental density

Detecting galaxy clusters in the redshift desert:

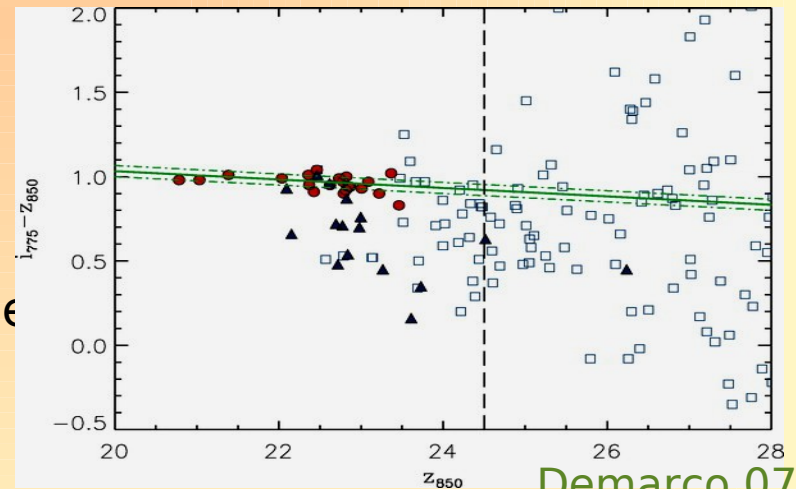
1) To distinguish heredity and environment in the evolution of galaxy properties:

- Segregation of red galaxies through biased galaxy formation (“Nature scenario”)



- ...or because of environment-dependent effects (*Ram Pressure Stripping, Thermal Evaporation, Turbulent/Viscous Stripping, Tidal Truncation, Harassment* etc.) (“Nurture scenario”)

2) To have a complete knowledge on the formation/evolution of red sequence galaxies and brightest cluster galaxies, a crucial test for galaxy evolution models.



3) To infer cosmological parameters from the evolution of the cluster mass function.

Cluster detection at high redshift ($z > 1$)

Various cluster detection techniques are currently employed:

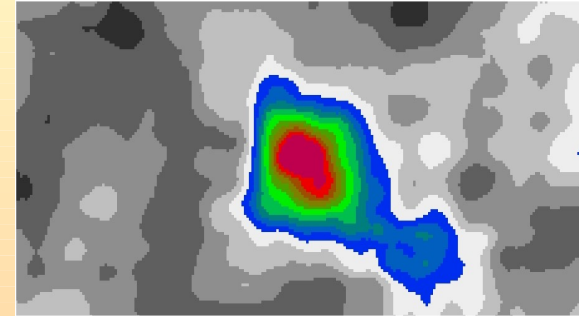
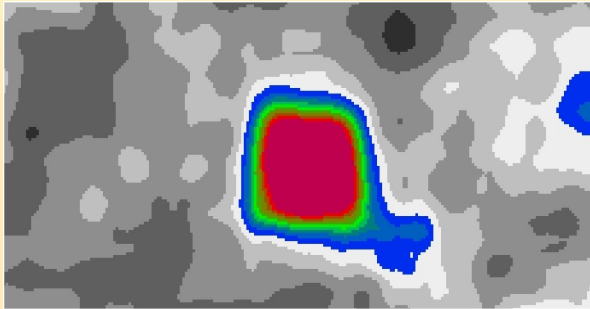
- **X-ray detections** (*e.g. Rosati 04, Mullis 05, Stanford 06, Lidman 08*)
- **SZ maps** (*e.g. Staniszewski 08*)
- **Red Sequence methods** (*e.g. Gladders&Yee 05, Goto 08, Andreon 08*)
- **Targeted searches** (*high-z radio gal., e.g. Venemans 07, Pentericci et al. 05, QSOs, e.g. Kashikawa 07*)
- **LBG clustering** (*e.g. Steidel 99, Peter 07, Ota 08*)

selecting clusters as galaxy overdensities in redshift space allows unbiased selection up to the highest redshifts: it is not dependent on virialisation status, on the presence of the red sequence or of an early type population.

The use of photometric redshifts allows to reach the deepest limits in multi-wavelength surveys.

Several studies in these last years explore cluster detection through photo-z: *Botzler 2004, Scoville 07, Zatloukal 07, Mazure 07, Eisenhardt 08, Kovac 09, van Breukelen 09.*

Galaxy Space Densities through photometric redshifts



We developed a method to detect overdensities using photometric redshifts (**Trevese et al. 2007 A&A 463**).

We divide the survey volume in cells ($\Delta\alpha=\Delta\delta =2.4$ arcsec and $\Delta z=0.025$) and for each cell we count neighbouring objects in progressively larger volumes. When a given number of neighbour is reached ($n=15$) the density to th cell is assigned as:

$$\rho = \frac{V}{n}$$

We take into account the increase of limiting luminosity with increasing redshift assigning a weight $w(z)$ to each object:

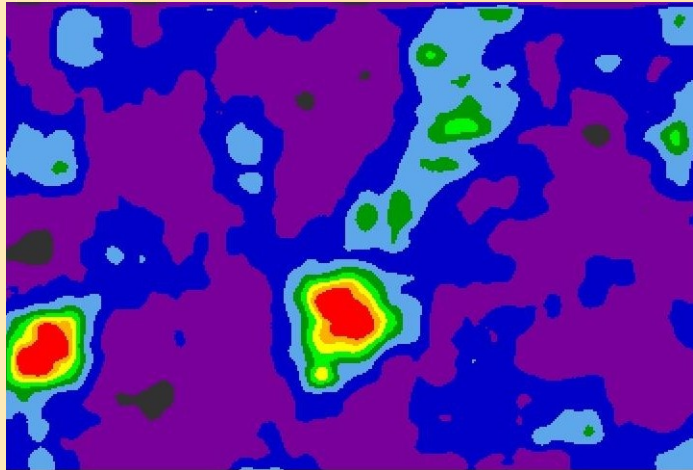
$$\frac{1}{w(z)} = \frac{\int \Phi(M) dM}{\int \Phi(M) dM}$$

Where $\Phi(M)$ is the redshift dependent galaxy LF determined from the GOODS-MUSIC catalog, On the basis of this we assume a reference redshift z_c below which we detect all objects brighter than the relevant $M_c \equiv M_{\text{lim}(z_c)}$

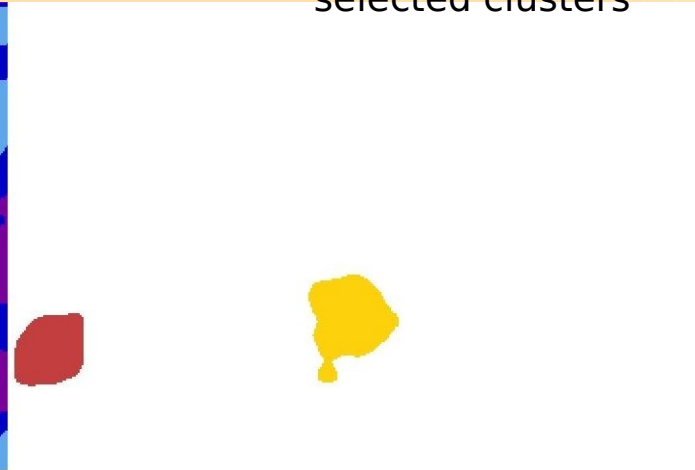
Cluster detection, tests and simulations

Structures are identified as connected regions with a density $\rho > \rho_{\text{med}} + 4\sigma$ and must have at least 15 members

FITS image of the density field



FITS image with the 'segmentation' of selected clusters



We tested our algorithm on simulations. In a deep survey like the GOODS field we can obtain reliable samples of clusters selected as 4σ regions of the density field

$(1.8 < z < 2.5)$

Purity

~75%

Completeness

~35%

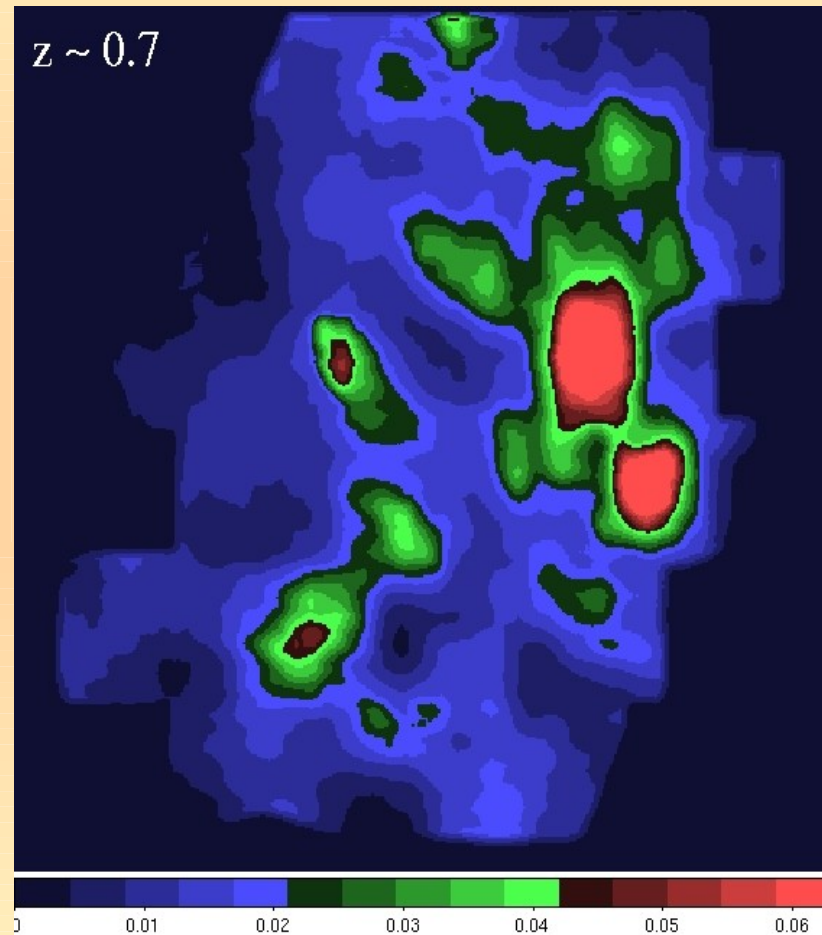
Low Redshift ($z < 1.8$) *High Redshift*

~95%

~85%

Clusters in the GOODS-South Field

We built a comprehensive catalogue of structures in the GOODS-South field up to $z \sim 2.5$ (Salimbeni et al. 2009). We find over-densities at $z \sim 0.7$ at $z \sim 1$, at $z \sim 1.6$ and $z \sim 2.2$:

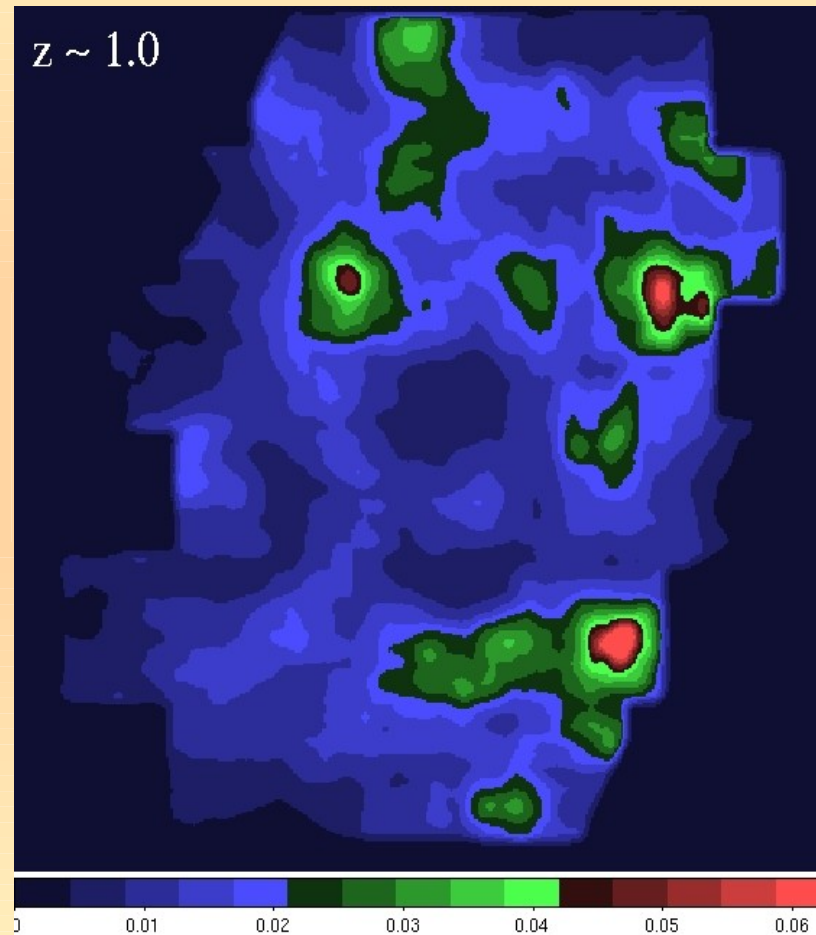


Spectroscopically confirmed.

Density maps at increasing redshift

Clusters in the GOODS-South Field

We built a comprehensive catalogue of structures in the GOODS-South field up to $z \sim 2.5$ (Salimbeni et al. 2009). We find over-densities at $z \sim 0.7$ at $z \sim 1$, at $z \sim 1.6$ and $z \sim 2.2$:

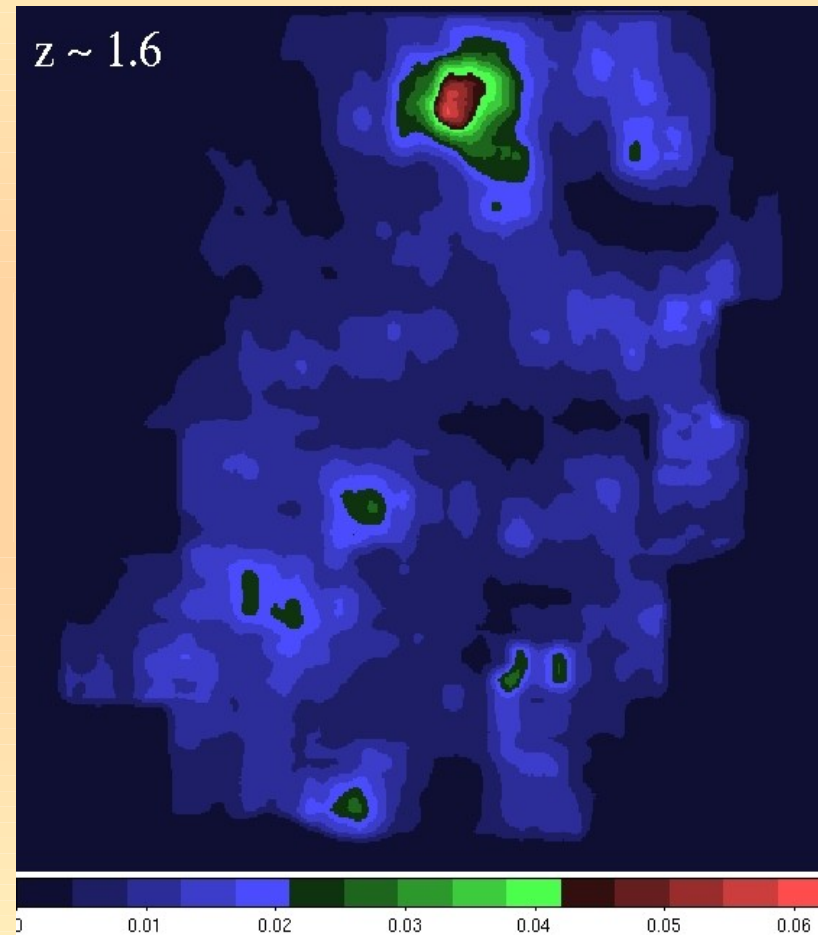


Two clusters are spectroscopically confirmed.

Density maps at increasing redshift

Clusters in the GOODS-South Field

We built a comprehensive catalogue of structures in the GOODS-South field up to $z \sim 2.5$ (Salimbeni et al. 2009). We find over-densities at $z \sim 0.7$ at $z \sim 1$, at $z \sim 1.6$ and $z \sim 2.2$:

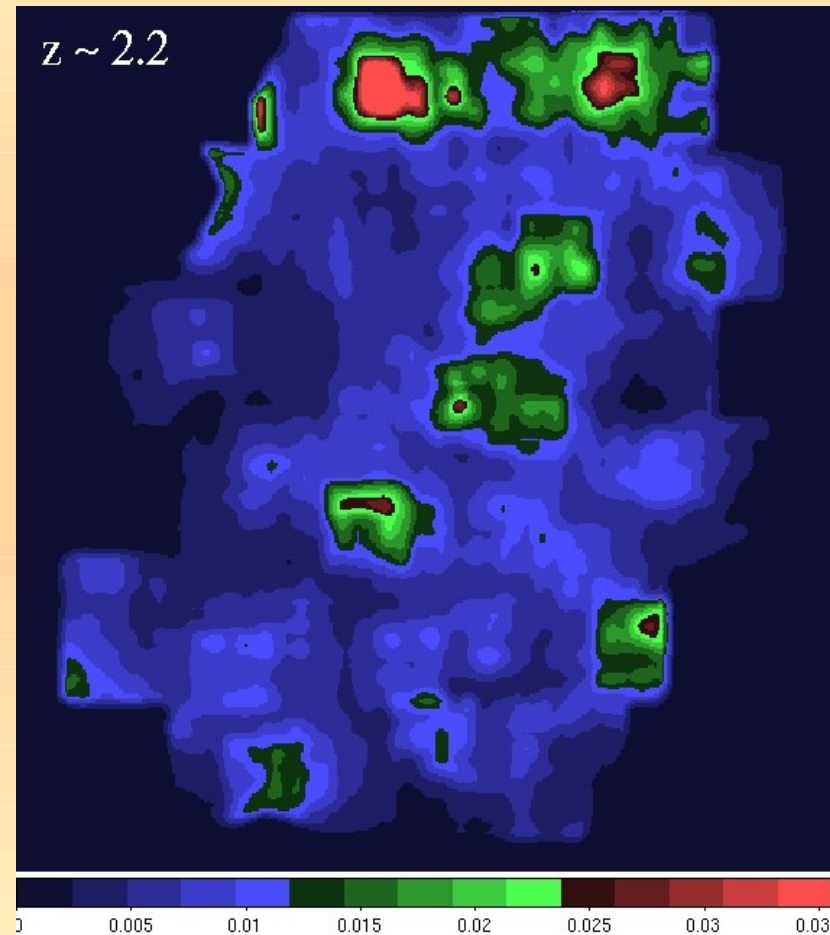


*Spectroscopically confirmed
(Kurk et al. 09)*

Density maps at increasing redshift

Clusters in the GOODS-South Field

We built a comprehensive catalogue of structures in the GOODS-South field up to $z \sim 2.5$ (Salimbeni et al. 2009). We find over-densities at $z \sim 0.7$ at $z \sim 1$, at $z \sim 1.6$ and $z \sim 2.2$:



MOS spectroscopic observations will be performed in 10 days with GEMINI South

Density maps at increasing redshift

For each structure we determine the mass from the overdensity following Steidel et al.1998 as $M = \rho_{\text{med}} V(1 + \delta_m)$ and $1 + \delta_m = 1 + \delta_{\text{gal}}/b$
Spectroscopic members (from public catalogues) were also identified to determine the velocity dispersion when possible

Table 6.1: Overdensities in the GOODS-South field.

ID	Redshift	RA J2000	DEC J2000	Members	Field	$M_{200}(M_{\odot}/10^{14})$ b=1-2	r_{200} Mpc b=1-2	Peak Overdensity σ_{ρ}
1	0.66	53.1623	-27.7913	19	6	0.3-0.15	1.1-0.9	7
2 ^a	0.66	53.0630	-27.8280	50	17	0.4-0.2	1.3-1.1	10
3	0.69	53.1690	-27.8747	54	20	0.5-0.3	1.4-1.1	6
4 ^{a,b,c}	0.71	53.0797	-27.7920	92	37	3.0-0.9	2.4-1.7	10
5	0.96	53.0843	-27.9020	32	14	*	*	6
6 ^c	1.04	53.0570	-27.7693	57	31	1.1-0.5	1.8-1.4	8
7	1.04	53.1577	-27.7660	60	26	0.8-0.4	1.6-1.2	6
8 ^{b,d}	1.06	53.0697	-27.8773	38	18	0.5-0.2	1.3-1.1	10
9 ^e	1.61	53.1270	-27.7140	50	24	4.9-2.0	2.9-2.1	7
10	2.23	53.0763	-27.7060	20	8	1.4-0.8	1.9-1.5	6
11	2.28	53.1470	-27.7087	23	12	1.3-0.6	1.8-1.5	10
12	2.28	53.0970	-27.7640	19	7	1.6-0.6	2.0-1.3	9

a - Gilli et al. (2003)

b - Adami et al. (2005)

c - Trevese et al. (2007)

d - Díaz-Sánchez et al. (2007)

e - Castellano et al. (2007)

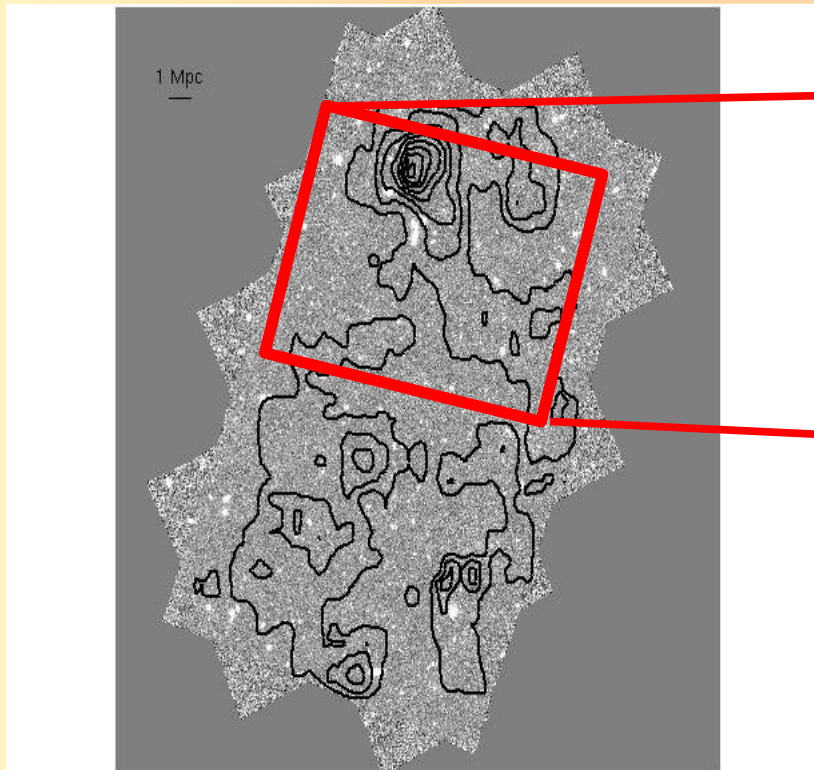
*-Note that we do not present M_{200} and r_{200} for structure 5 because it is located on the edge of the field and it is very near to structure 8.

A forming cluster at $z \sim 1.6$

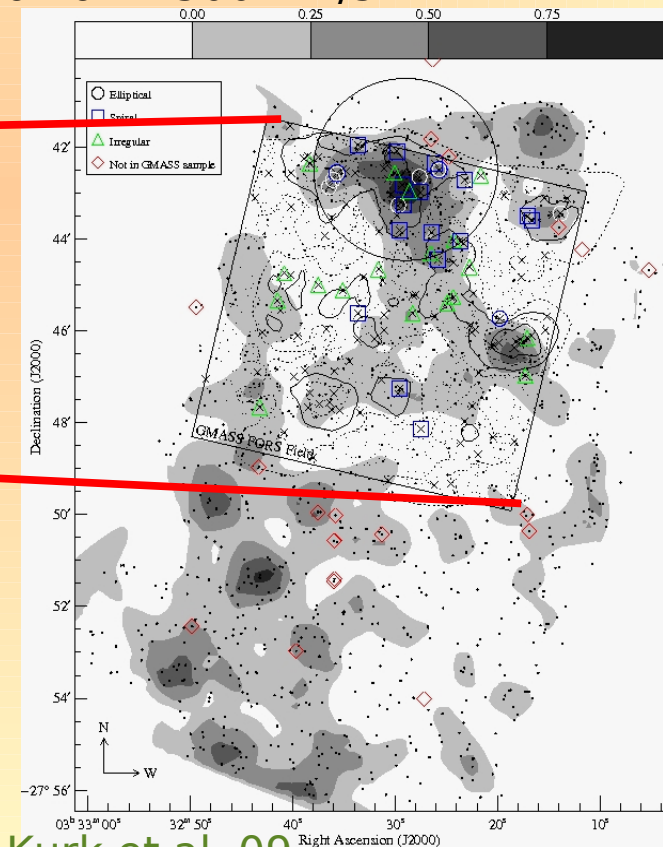
We analysed in depth the forming cluster at $z \sim 1.6$ (RA=03^h 32^m 29.28^s, DEC=-27° 42' 35.99") (Castellano et al. 2007). It is embedded in a diffuse structure at $z \sim 1.61$.

We estimate an M_{200} mass in the interval $1.3 \times 10^{14} - 5.7 \times 10^{14} M_{\text{sun}}$

The cluster has been subsequently spectroscopically confirmed in the context of the GMASS survey (Kurk et al. 2009): velocity dispersion of ~ 500 Km/s

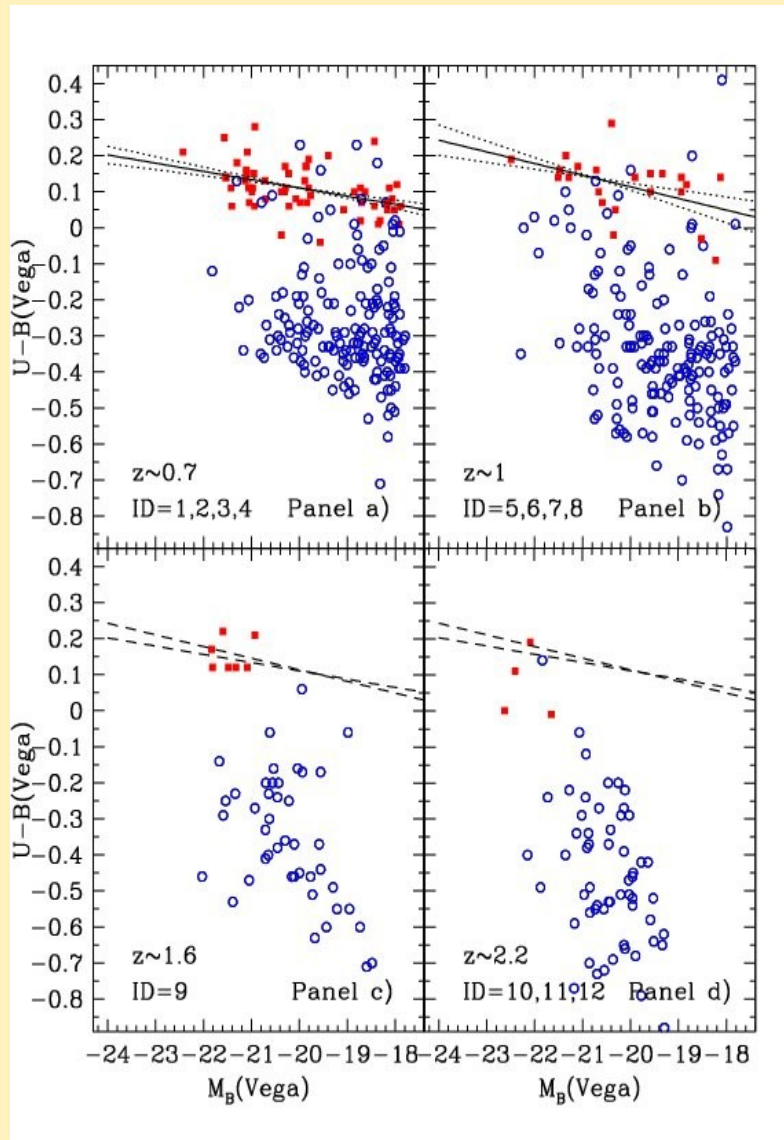


Castellano et al. 07



Kurk et al. 09

Rest Frame Colour-Magnitude diagrams



C-M diagrams for galaxies in different overdensities

:
Red = objects that have $\text{Age}/\tau > 4$ from SED fitting and are presumably passively evolving galaxies
Blue : starforming galaxies

- No evolution of the slope up to $z \sim 1$
- No clear indication of slope evolution at $z \sim 1.6$
- At $z \sim 2.2$ there is not evidence for a red sequence. "Red" galaxies are bluer than expected.

X-ray properties

The two most massive groups ($z \sim 0.7$ and $z \sim 1.6$) are X-ray underluminous if we place them in a standard M_{200} - L_X diagram for X-ray selected clusters. (Masses are estimated from the galaxy density contrast according to Steidel et al. 1998)

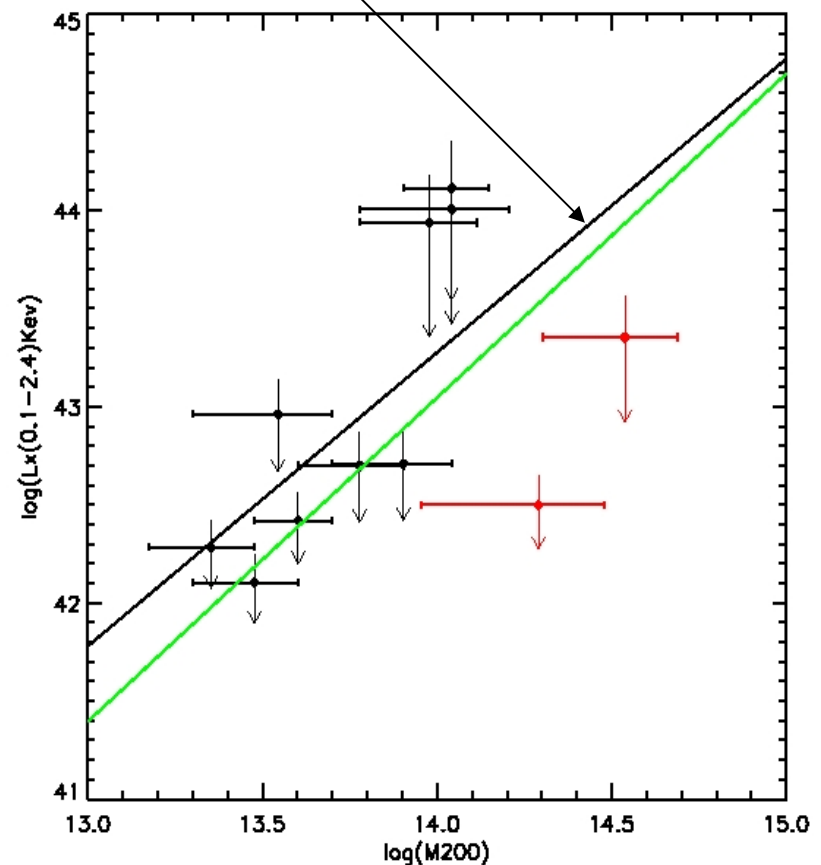
Best fit relations found from X-ray detected clusters by **Reiprich 08** and **Rykoff 02**

Table 5. X-ray observations.

ID	Count Rate 0.3–4 keV (10^{-5})	Flux ^a 0.5–2 keV (10^{-16} erg s ⁻¹ cm ⁻²)	L_X ^a 0.1–2.4 keV (10^{43} erg s ⁻¹)	S/N ^b
1	8.49	6.80–9.01	0.12–0.26	u.l.
2	5.56	4.45–5.90	0.08–0.18	u.l.
3	10.1	8.15–10.98	0.16–0.37	u.l.
4	11.2	9.04–12.31	0.19–0.44	u.l.
5	23.7	19.31–29.21	0.86–2.36	11.3
6	5.90	3.04–4.14	0.26–0.76	u.l.
7	5.77	2.97–4.05	0.26–0.74	u.l.
8	9.88	5.10–6.91	0.47–1.37	u.l.
9	5.68	3.08–4.14	0.83–3.67	u.l.
10	9.37	5.39–7.54	3.50–22.43	u.l.
11	5.72	3.29–4.69	2.27–15.06	u.l.
12	6.70	3.85–5.50	2.66–17.64	u.l.

^a Values for a Raymond-Smith model with assumed temperature respectively of 3 keV and 1 keV and metallicity $0.2 Z_{\odot}$.

^b u.l. indicates structures with a 3σ upper limit in the flux.

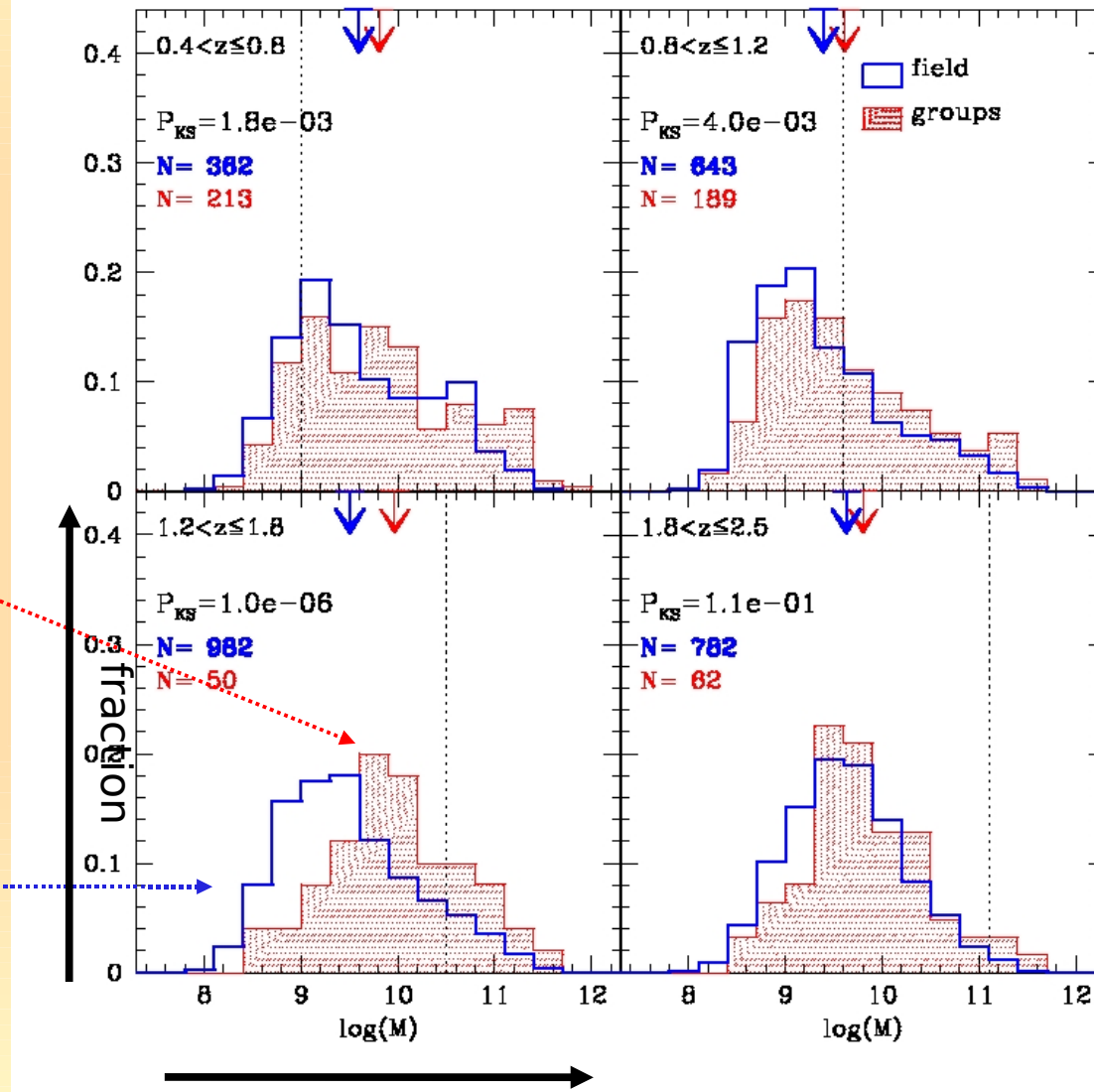


Galaxy properties as a function of density - II

We find that galaxies at high densities have a distribution that peaks at higher masses

Cluster Galaxies

Field Galaxies

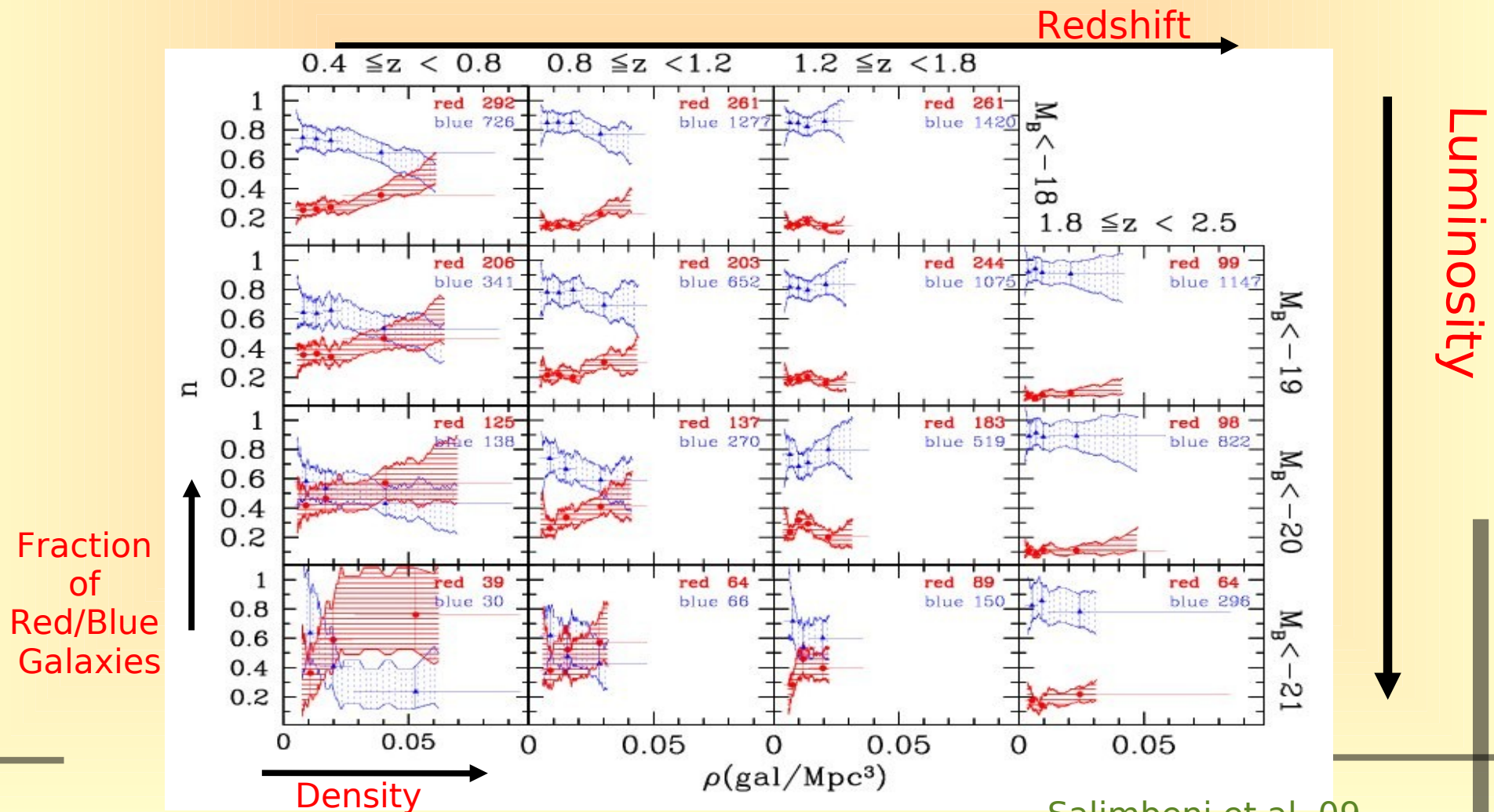


log(Mass)

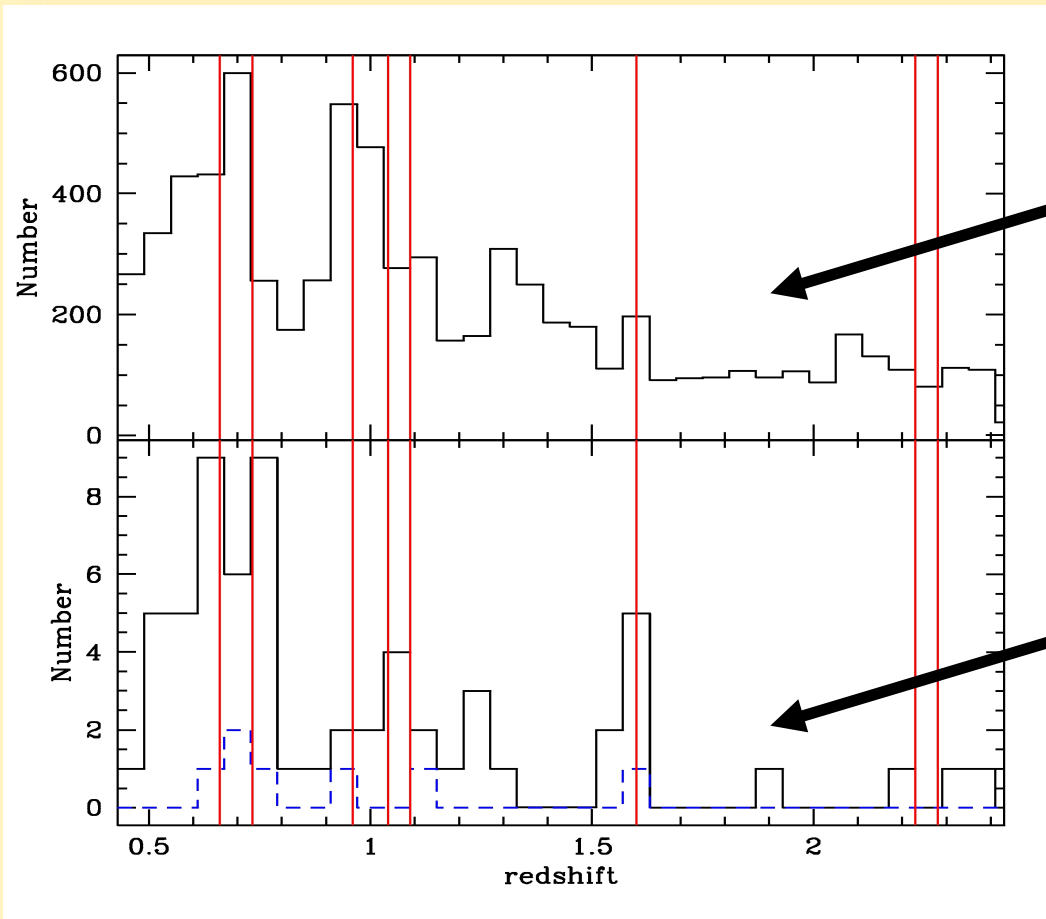
Salimbeni et al. 09

Galaxy properties as a function of density - III

We separate red and blue galaxies using the minimum in the bimodal distribution in the (U-V) vs B color magnitude diagram (Salimbeni et al. 2008). We determine how the fraction of red/blue galaxies changes with density at various luminosity and redshift. The color segregation progressively disappears at high redshift.



The relation between AGNs and cluster/LSS



Redshift Distribution of spectroscopic galaxies.

Redshift Distribution of spectroscopically confirmed AGNs.

Red lines mark the position of groups and clusters.

[AGNs trace the large scale structure.](#)

The relation between AGNs and cluster/LSS

We searched for AGNs in the clusters/groups at $0.7 < z < 1$ by cross correlating our catalogue of cluster members with the Luo et al. (2008) Chandra 2 Msec sources and the VLA source catalog of the CDF (Miller et al. 2008)

Sources with $HR \geq -0.2$ are classified as type 2 AGN
 $HR < -0.2$ and $L_x > 10^{42}$ are type 1 AGN
 $HR < -0.2$ and $L_x < 10^{42}$ are galaxies

we find a total 13 type 2 AGN 1 type 1 AGN + 2 radio sources in all galaxies down to $M = -20$ (140 galaxies)

Percentage = 12% → Higher than the analogous AGN fraction in massive clusters at similar redshift (Martini 2009)

We note that the groups with higher AGN fraction ($>$ median value) have a velocity distribution that is bimodal

While groups/cluster with low AGN fraction have a smoother velocity distribution

The only group with a smooth-extended Xray emission from hot cluster gas (indicative of virialization) has no AGN

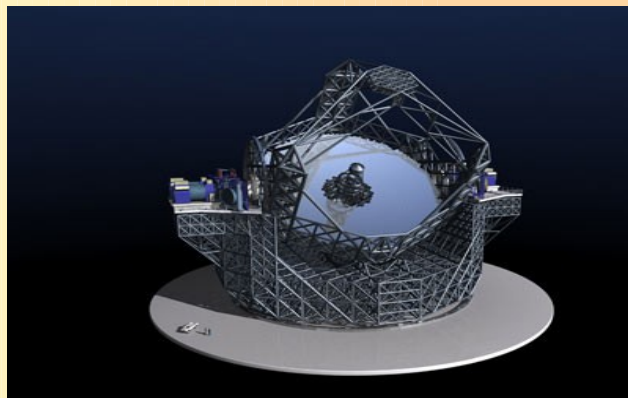
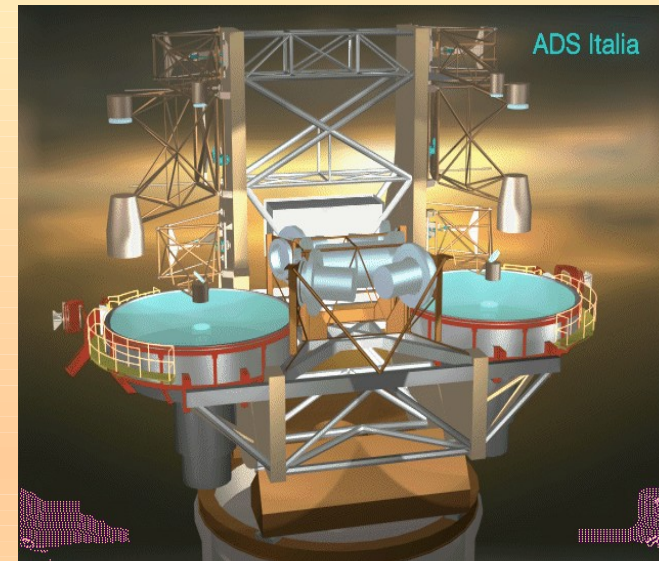
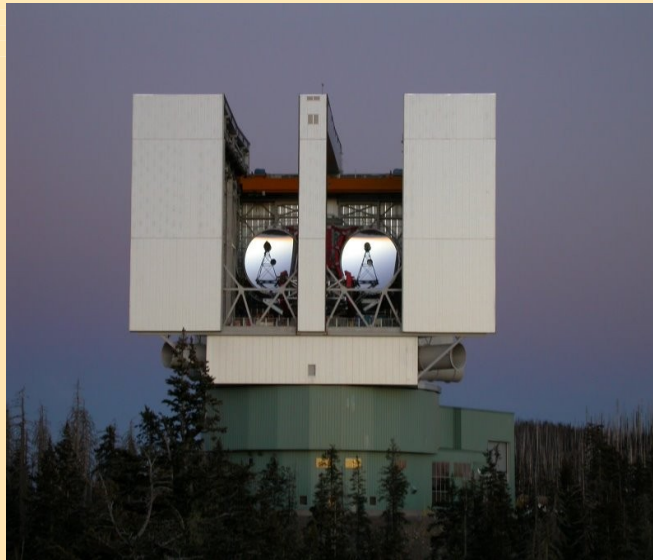
[Presence of AGNs might be related to virialisation status?](#)

Conclusions

- It is possible to study high redshift galaxy environment, and to individuate galaxy clusters, with photometric redshifts.
- We built a comprehensive **catalogue of structures in the GOODS-South field**. 'Sheets' of diffuse overdensities, with embedded groups/clusters, appear up to the highest redshifts probed.
- Among them we **detected an high redshift small cluster** later confirmed with spectroscopy. It shows the characteristics of a **forming cluster** and a forming red sequence.
- The most massive clusters in our sample seem to be X-ray underluminous.
- We found that **color segregation** with density is higher at lower redshift and brighter magnitudes but it **seems to disappear, also for the brightest galaxies, between $z \sim 1.5$ and $z \sim 2.0$** .

FUTURE APPLICATIONS?

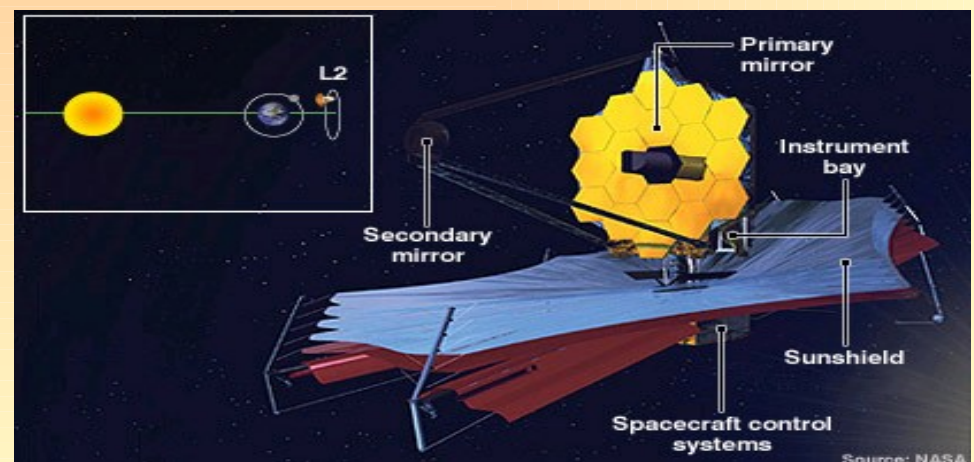
Deep optical/near IR surveys with facilities like LBT, WFC3(@HST), VISTA(@VLT), EELT, JWS



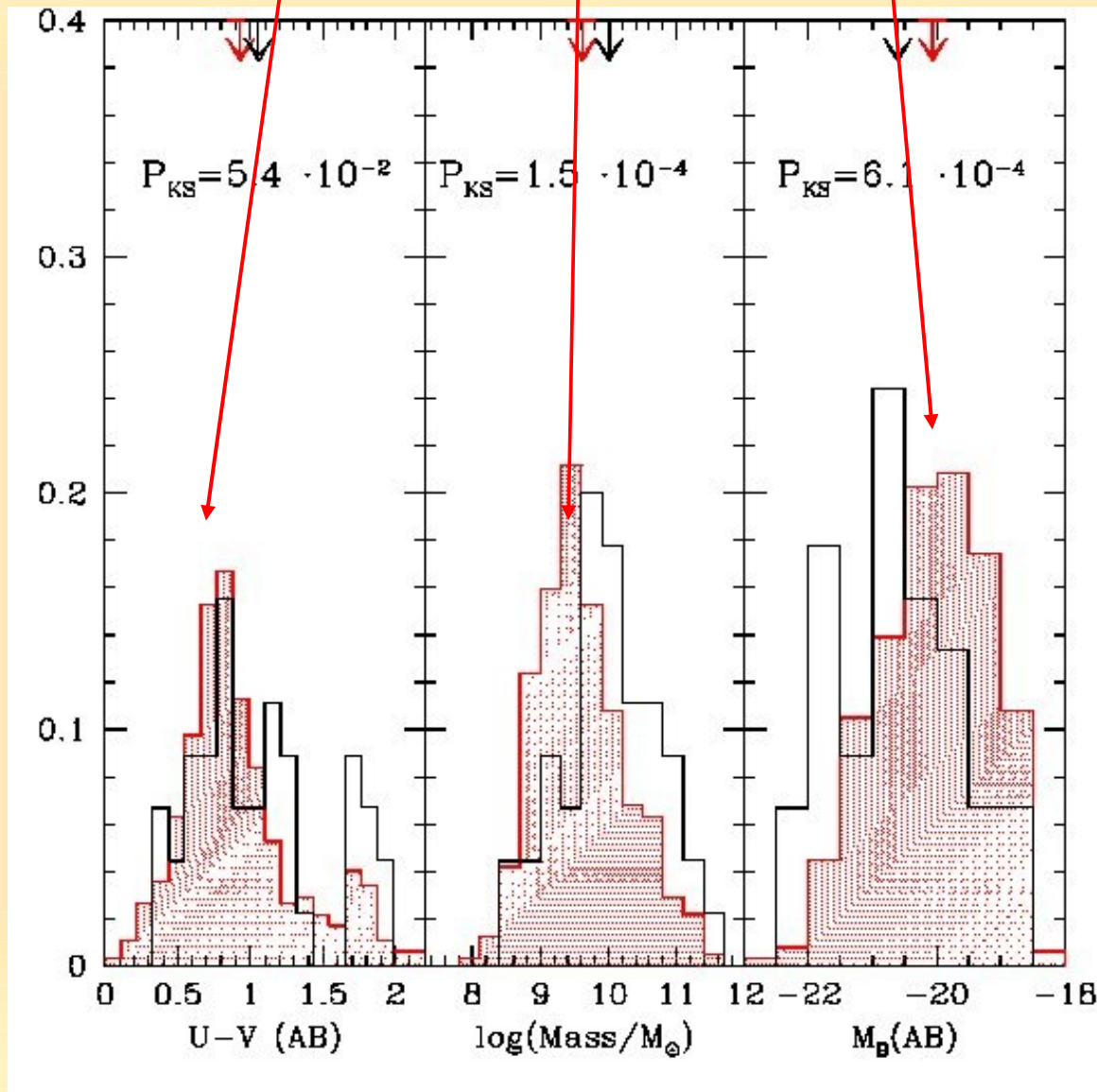
The European Extremely Large Telescope
(Artist's Impression)

ESO PR Photo 46/06 (11 December 2006)

© ESO

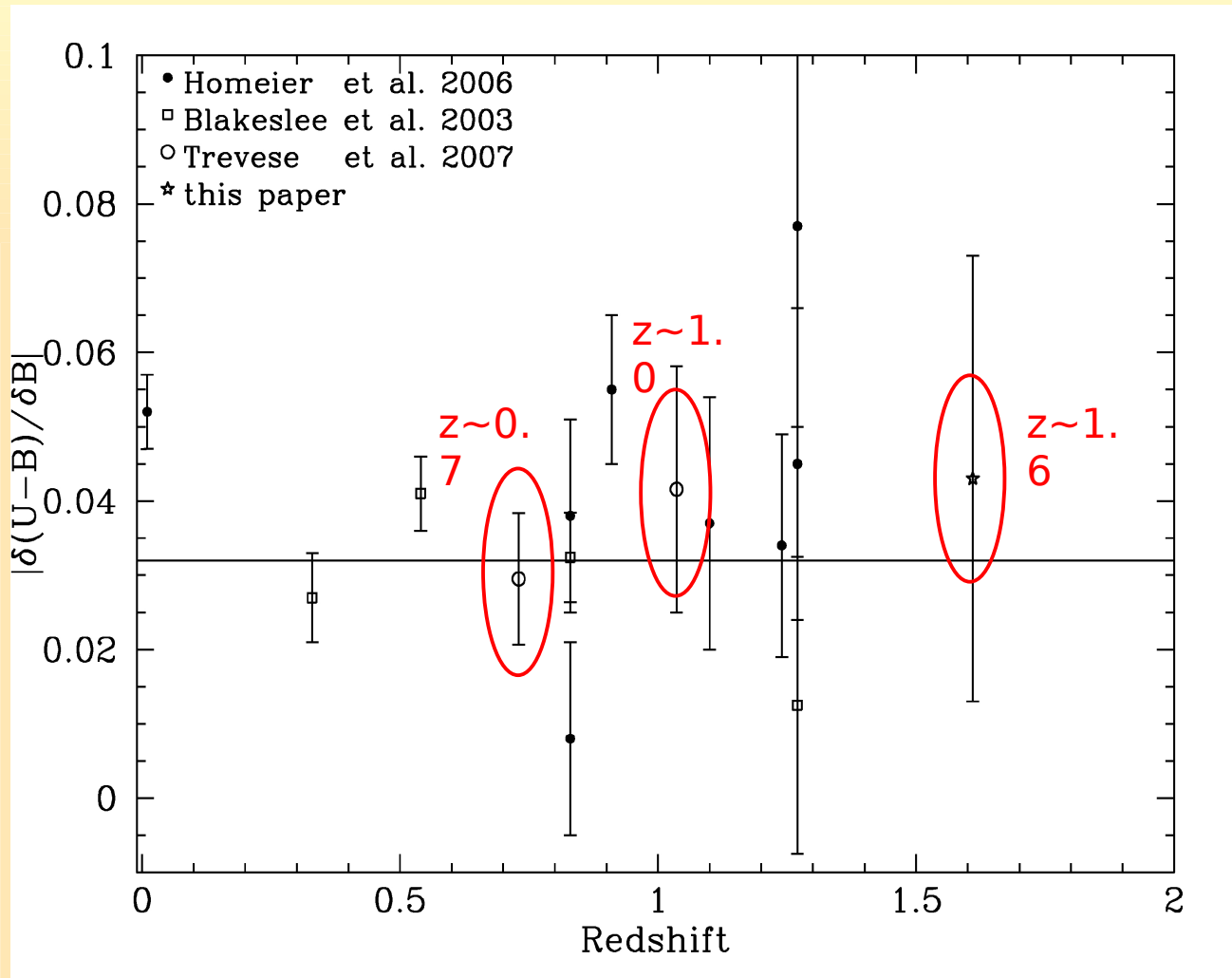


Galaxies are, on average, redder, more massive and more luminous than 'field' galaxies at the same redshift.



9 of its galaxies form a nascent red sequence

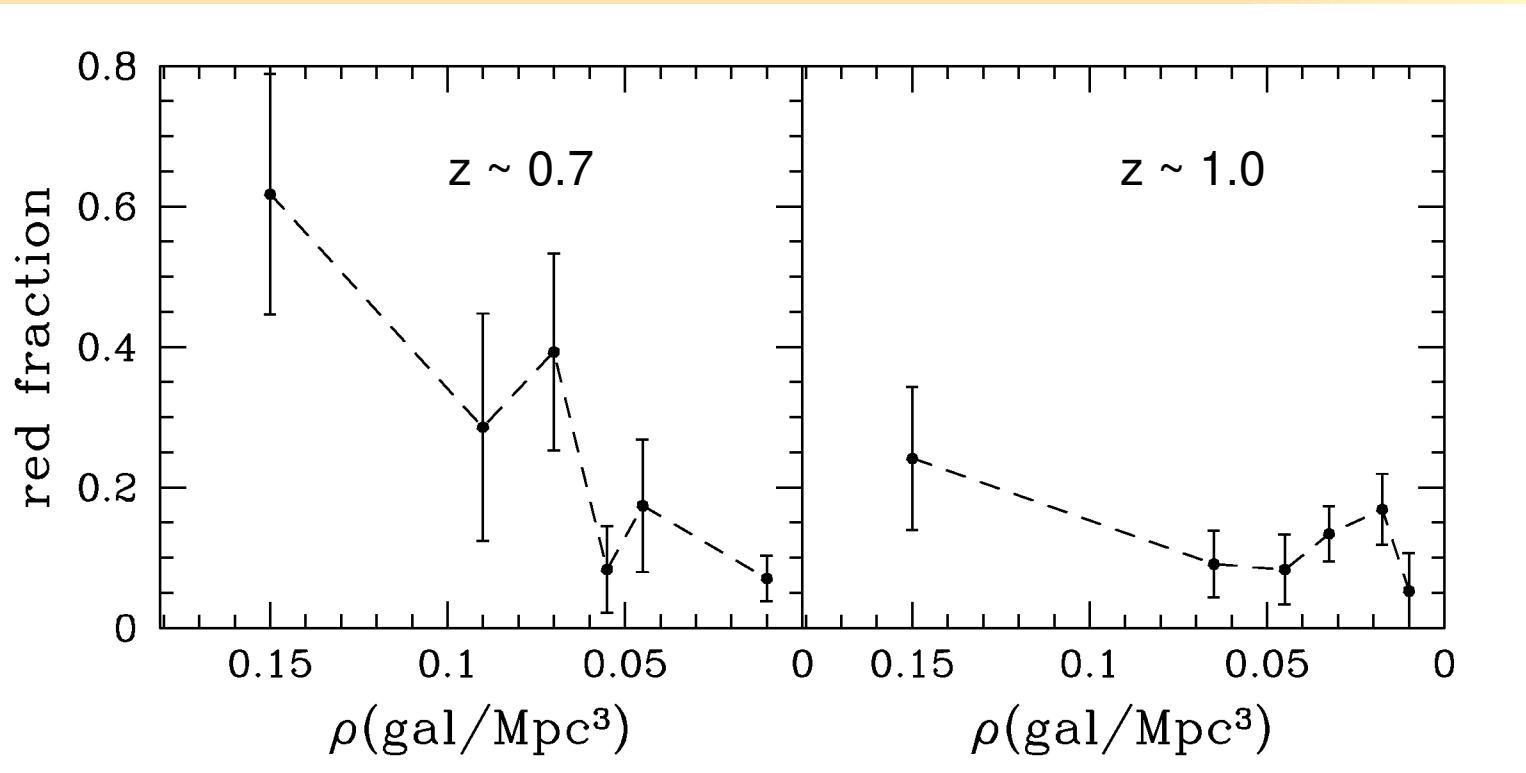
Castellano et al. 08



The red sequence slope seems constant up to high redshift: comparison with values from the literature, but the data (and the objects are very few).

Selecting galaxies inside and outside two groups of similar galaxy richness (at $z \sim 0.7$ and $z \sim 1$) we find that the fraction of red cluster galaxies has greatly decreased in less than 2.0 Gyr .

Fraction of Red Galaxies



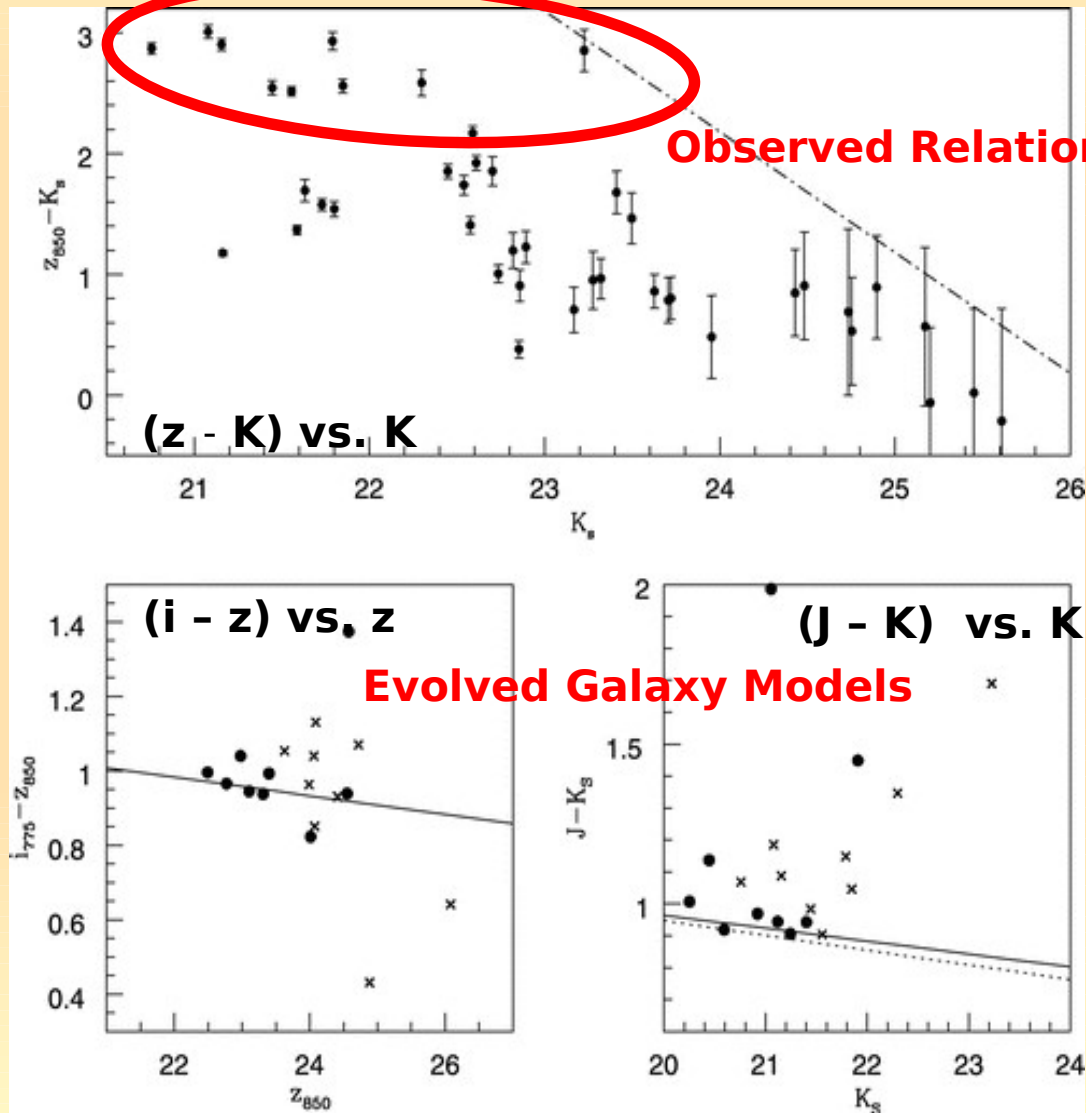
←

Density

Trevese et al. 2007

A forming cluster at $z \sim 1.6$ - C-M diagram

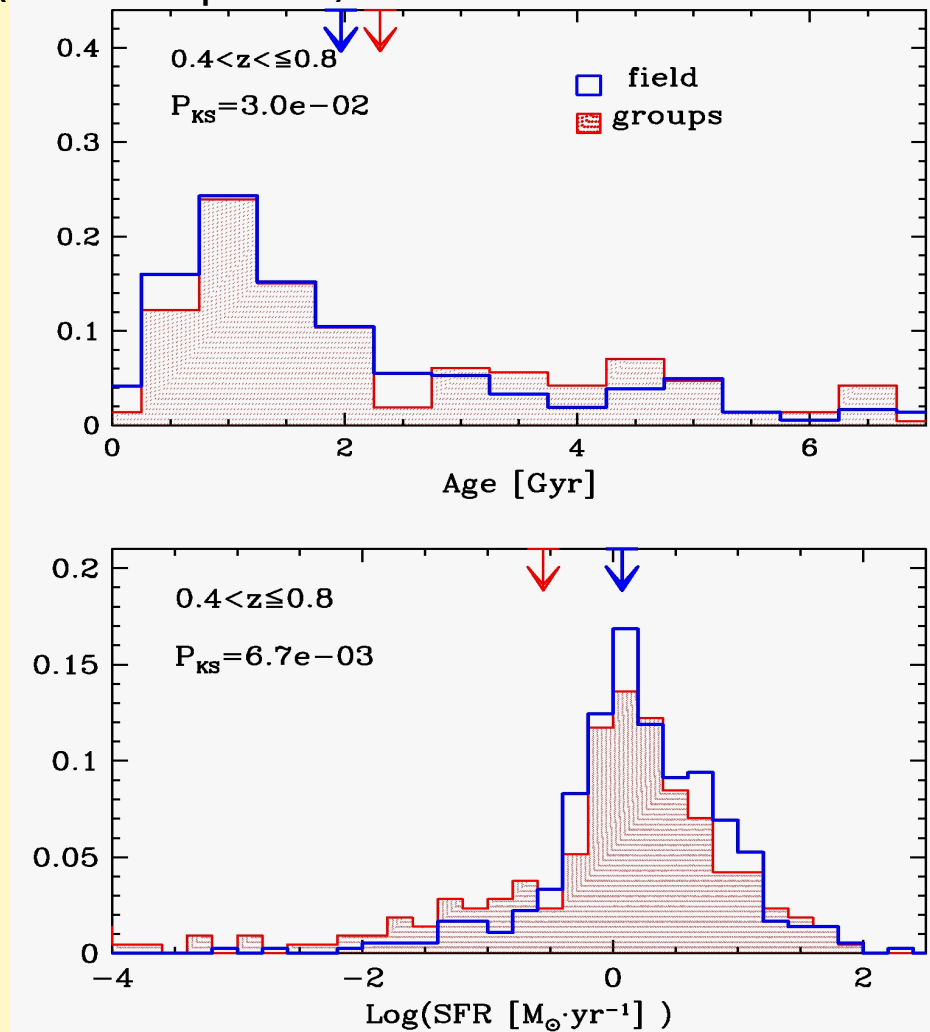
As we evolve the colors of the 9 reddest galaxies we find a good agreement with the red sequence of a spectroscopically detected massive cluster at $z = 1.24$ (e.g. De Marco et al. 2007).



Castellano et al. 07

Galaxy properties as a function of density - I

At low redshift ($0.4 < z < 0.8$) we find differences as a function of the environment in the distribution of **galaxy ages** (upper panel) and **star formation rates** (bottom panel).



- cluster-group galaxies are on average older than field galaxies

- In the cluster/group sample there is a higher fraction of galaxies with low SFR